TOXICOLOGICAL SCIENCES, 164(2), 2018, 489–500

doi: 10.1093/toxsci/kfy099
Advance Access Publication Date: April 20, 2018
Research Article

Metabolism and Toxicity of Trichloroethylene and Tetrachloroethylene in Cytochrome P450 2E1 Knockout and Humanized Transgenic Mice

Yu-Syuan Luo,* Shinji Furuya,* Valerie Y. Soldatov,† Oksana Kosyk,† Hong Sik Yoo,† Hisataka Fukushima,* Lauren Lewis,* Yasuhiro Iwata,* and Ivan Rusyn*,[1]

*Department of Veterinary Integrative Biosciences, Texas A&M University, College Station, Texas 77843; and †Department of Environmental Sciences and Engineering, University of North Carolina, Chapel Hill, North Carolina 27599

[1]To whom correspondence should be addressed. Fax: (979) 458-9866. E-mail: irusyn@cvm.tamu.edu.

ABSTRACT

Trichloroethylene (TCE) and tetrachloroethylene (PCE) are structurally similar olefins that can cause liver and kidney toxicity. Adverse effects of these chemicals are associated with metabolism to oxidative and glutathione conjugation moieties. It is thought that CYP2E1 is crucial to the oxidative metabolism of TCE and PCE, and may also play a role in formation of nephrotoxic metabolites; however, inter-species and inter-individual differences in contribution of CYP2E1 to metabolism and toxicity are not well understood. Therefore, the role of CYP2E1 in metabolism and toxic effects of TCE and PCE was investigated using male and female wild-type [129S1/SvlmJ], *Cyp2e1*(−/−), and humanized *Cyp2e1* [*hCYP2E1*] mice. To fill in existing gaps in our knowledge, we conducted a toxicokinetic study of TCE (600 mg/kg, single dose, *i.g.*) and a subacute study of PCE (500 mg/kg/day, 5 days, *i.g.*) in 3 strains. Liver and kidney tissues were subject to profiling of oxidative and glutathione conjugation metabolites of TCE and PCE, as well as toxicity endpoints. The amounts of trichloroacetic acid formed in the liver was *hCYP2E1*≈ 129S1/SvlmJ > *Cyp2e1*(−/−) for both TCE and PCE; levels in males were about 2-fold higher than in females. Interestingly, 2- to 3-fold higher levels of conjugation metabolites were observed in TCE-treated *Cyp2e1*(−/−) mice. PCE induced lipid accumulation only in liver of 129S1/SvlmJ mice. In the kidney, PCE exposure resulted in acute proximal tubule injury in both sexes in all strains (*hCYP2E1* ≈ 129S1/SvlmJ > *Cyp2e1*(−/−)). In conclusion, our results demonstrate that CYP2E1 is an important, but not exclusive actor in the oxidative metabolism and toxicity of TCE and PCE.

Key words: trichloroethylene; tetrachloroethylene; cytochrome P450 2E1; toxicokinetics; toxicodynamics.

Trichloroethylene (TCE) and tetrachloroethylene (PCE) are structurally similar olefins and high-production volume chemicals that have been used in chemical synthesis, metal degreasing, dry cleaning, and other industrial applications (U.S. EPA, 2011a,b). TCE and PCE are extensively present in air, soil, and surface and ground water supplies (IARC, 2014). They are also frequently found at the hazardous waste sites on the National Priorities List (ATSDR, 2014). TCE and PCE are also detectable in human blood samples collected in the National Health and Nutrition Examination Survey (Jia *et al.*, 2012). TCE and PCE are classified as "carcinogenic to humans" and "probably carcinogenic to humans," respectively, by the International Agency for Research on Cancer (Guha *et al.*, 2012). They also can cause non-cancer effects in liver and kidney (Cichocki *et al.*, 2016). TCE and PCE are among the top 10 chemicals of concerns for the risks to human health and environment under the revised Toxic Substances Control Act (U.S. EPA, 2017).

Tissue-specific toxicity of TCE and PCE results from metabolism through the oxidative and glutathione (GSH) conjugation pathways (Figure 1). Oxidation of TCE and PCE occurs on the

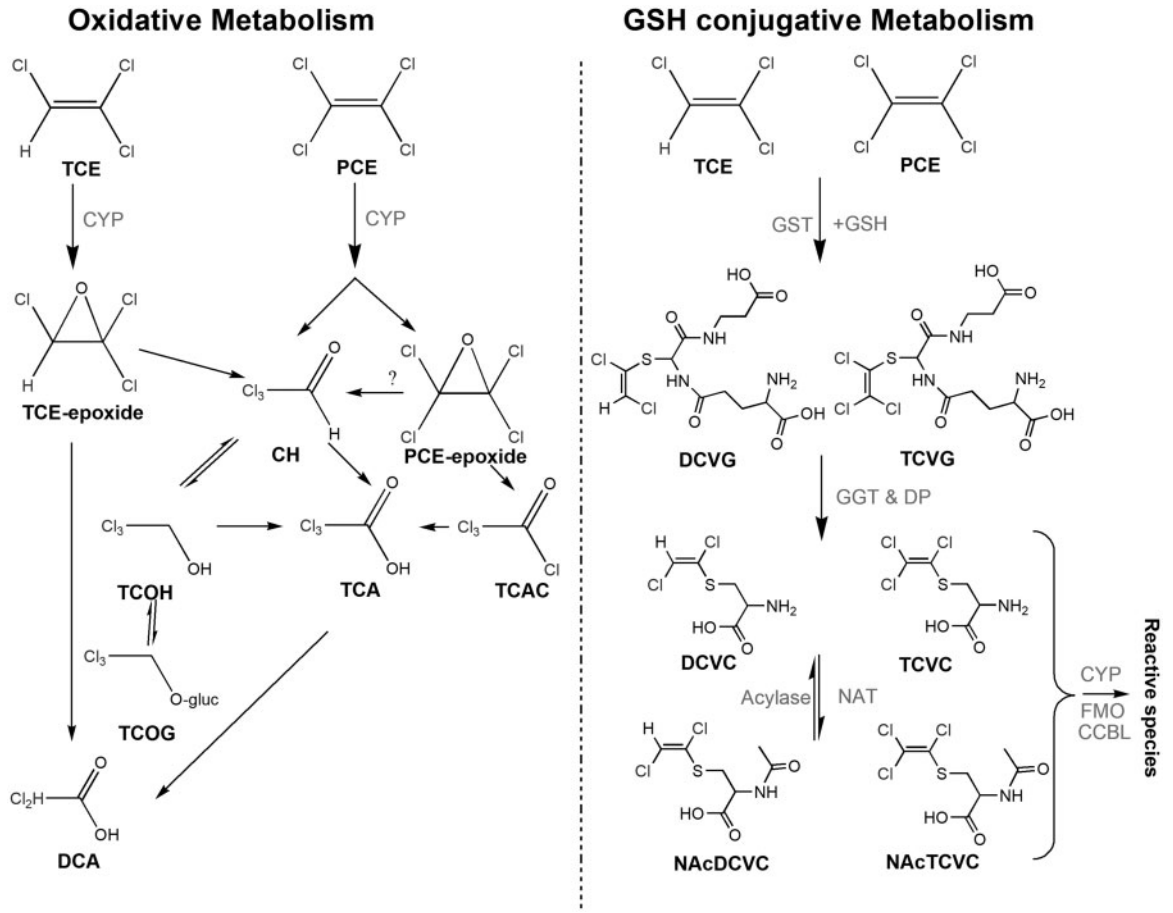

Figure 1. Overview of the metabolic pathways of TCE and PCE. Upon absorption, TCE and PCE can either be oxidized via CYPs or conjugated with GSH via GSTs. Abbreviations: TCE, trichloroethylene; PCE, tetrachloroethylene; CH, chloral hydrate; TCOH, trichloroethanol; TCA, trichloroacetate; TCAC, trichloroacetyl chloride; TCOG, trichloro-glucuronide conjugate; DCA, dichloroacetate; DCVG, S-(1, 2-dichlorovinyl)-GSH; DCVC, S-(1, 2-dichlorovinyl)-cysteine; NAcDCVC, N-acetyl-S-(1, 2-dichlorovinyl)-cysteine; TCVG, S-(1, 2, 2-trichlorovinyl)-GSH; TCVC, S-(1, 2, 2-trichlorovinyl)-cysteine; NAcTCVC, N-acetyl-S-(1, 2, 2-trichlorovinyl)-cysteine; GGT, gamma-glutamyl transferase; DP, dipeptidase; NAT, n-acetyl transferase; FMO, flavin monooxygenase; CCBL, cysteine conjugate beta-lyase.

double bond via cytochrome P450s (CYPs) to form an epoxide intermediate, which is subsequently metabolized to oxidative species, including trichloroacetic acid (TCA) and/or TCE-specific metabolite trichloroethanol (TCOH) (Cichocki *et al.*, 2016). TCA is a ligand to mouse and human peroxisome prliferator-activated receptor alpha (PPARα) (Zhou and Waxman, 1998), which may be associated with cell proliferation in liver (Laughter *et al.*, 2004). Both TCE and PCE are also metabolized by GSH conjugation via GSH-S-transferases (GSTs) to generate dichloro- or trichloro-GSH conjugates (DCVG/TCVG) (Lash *et al.*, 2000). These conjugates can be further metabolized by hepatic or renal gamma glutamyl transferase and dipeptidase to form cysteine conjugates (S-(1, 2-dichlorovinyl)-cysteine [DCVC]/ S-(1, 2, 2-trichlorovinyl)-cysteine [TCVC]), and then are subject to n-acetylation to form NAcDCVC or NAcTCVC. These can be further bio-activated by a number of enzymes, including cysteine s-conjugate beta lyase, flavin monooxygenase, and CYPs, to form nephrotoxic metabolites such as reactive thiols (Volkel and Dekant, 1998) and sulfoxides (Elfarra and Krause, 2007; Lash *et al.*, 2001, 2003; Ripp *et al.*, 1997; Werner *et al.*, 1996). For both TCE and PCE, various CYPs play a critical role in generating metabolites that cause toxicity in both liver and kidney.

Among the CYPs isoenzymes, CYP 2E1 (CYP2E1) is the major contributor to oxidation of chlorinated solvents (Kim and Ghanayem, 2006; Nakajima *et al.*, 1993; Ramdhan *et al.*, 2008). CYP2E1 is highly variable in expression (12-fold) in human liver (Lin and Lu, 2001) and interindividual differences in CYP activity are thought to be a major contributor to population variability in adverse effects of TCE and PCE (Cichocki *et al.*, 2016). In studies with TCE, both hepatotoxicity and production of oxidative metabolites were ameliorated in CYP2E1 knockout mice (Kim and Ghanayem, 2006; Ramdhan *et al.*, 2008), albeit little is known about the exact role of CYP2E1 in TCE toxicokinetics. In experiments with PCE, one study posited that CYP2E1 can contribute to PCE toxicity (Hanioka *et al.*, 1995), but another study concluded that CYP2E1 is not the critical enzyme in sub-chronic effects of PCE (Philip *et al.*, 2007). No study examined metabolism or toxicity of PCE in CYP2E1 knockout or humanized mice.

Therefore, in this work, we aimed to address existing knowledge gaps on the role of mouse and human CYP2E1 in the metabolism and toxicity of TCE and PCE. Because several studies already established that CYP2E1 is playing a role in liver effects of TCE, but its precise role in the formation of TCE metabolites is largely unknown, we conducted a toxicokinetic study of TCE in male and female 129S1/SvlmJ, *Cyp2e1(−/−)*, and humanized *(hCYP2E1)* mice. For PCE, we aimed to test whether CYP2E1 plays a role in the toxicity of PCE by using the same genetic models and a sub-acute study design.

MATERIALS AND METHODS

Chemicals. TCE (purity ≥99.5%), PCE (≥99.9%), TCA (≥99.0%), TCOH (≥99.0%), 2-bromobutyric acid (≥97%), chloroform (≥99.9%), and formic acid (≥95%) were obtained from Sigma-Aldrich (St Louis, Missouri). Methanol (≥99.9%) was from Fischer Scientific (Hampton, New Hampshire). DCVC (≥98.0%), S-(1, 2-dichlorovinyl)-cysteine-$^{13}C_3$-^{15}N (DCVC*, purity ≥95.0%, isotopic purity ≥98.0%), S-(1, 2-dichlorovinyl)-GSH(DCVG, ≥98.9%), and S-(1, 2-dichlorovinyl)-GSH-$^{13}C_2$-^{15}N (DCVG*, purity ≥90.0%, isotopic purity ≥98.0%) were obtained from TLC Pharmaceutical Standards (Aurora, Canada). N-acetyl- (NAcDCVC, 99.8%), N-acetyl-S-(1, 2-dichlorovinyl)-cysteine-^{13}C, d_3 (NAcDCVC*, purity: 97.6%, isotopic purity: 99.0%), and NAcTCVC (purity: 99.7%) were purchased from Toronto Research Chemicals (Toronto, Canada). S-(1, 2, 2-trichlorovinyl)-GSH-$^{13}C_2$-^{15}N (TCVG*, purity: 90.4%), TCVC-$^{13}C_3$-^{15}N (TCVC*, purity: 97.5%), and N-acetyl-S-(1, 2-dichlorovinyl)-cysteine-$^{13}C_3$-^{15}N (NAcTCVC*, purity: 99.0%) were used as internal standards for TCVG, TCVC, and NAcTCVC, respectively. TCVG (purity: 98.9%), TCVC (purity: 98.4%), and all stable isotopically labeled internal standards were synthesized by Dr Avram Gold at the University of North Carolina at Chapel Hill.

Animals and treatments. Male and female wild type, *Cyp2e1(−/−)*, and *hCYP2E1* mice on 129S1/SvlmJ (Sv129, The Jackson Laboratory, Bar Harbor, Maine) were used in this study. Transgenic mice were bred and genotyped by PCR before being used in this study. The primer sequences are detailed in Supplementary Table 1. Mice were housed in polycarbonate cages on Sani-Chips irradiated hardwood bedding (P.J. Murphy Forest Products, Montville, New Jersey), and supplied with NTP-2000 (Zeigler Brothers, Gardners, Pennsylvania) wafer diet and water *ad libitum* on a 12 h light-dark cycle. After a week-long acclimatization, mice were intragastrically administered with TCE or PCE (Figure 2). All treatments and procedures were approved by the Institutional Animal Care and Use Committee at the University of North Carolina at Chapel Hill.

In a study of TCE toxicokinetics, mice were administered a single dose of 600 mg/kg TCE or vehicle (5% Alkamuls EL-620 in saline). The dose was selected based upon previous mouse studies showing that this amount was well tolerated in acute, 90-day, and 2-year studies (Buben and O'Flaherty, 1985; Luo *et al.*, 2018; National Toxicology Program, 1990; Yoo *et al.*, 2015a). In addition, mice form approximately 100-fold less GSH conjugation metabolites (Chiu *et al.*, 2009), which justifies the use of a dose that is higher than the environmental exposure to TCE. After dosing, mice were anesthetized (pentobarbital, 50 mg/kg i.p.) and sacrificed by exsanguination through the *vena cava* at 2, 5, 12, and 24 h (n = 2–4 per group per time point). Mice dosed with vehicle were sacrificed at 5 h after gavage. Livers and kidneys were collected, blotted dry, and snap-frozen in liquid nitrogen. Serum was prepared by using Z-gel tubes (Sarstedt, Darmstadt, Germany). All tissues and serum were stored at −80°C until analyzed.

In a study of PCE metabolism and toxicity, mice were treated for 5 days with single daily dose (9 AM) of 500 mg/kg/day PCE or vehicle (5% Alkamuls EL-620 in saline). The dose was selected based upon previous studies showing no saturation of PCE oxidation at similar doses (Buben and O'Flaherty, 1985; Philip *et al.*, 2007), and that this amount was well tolerated in acute, 90-day, and 2-year studies (Buben and O'Flaherty, 1985; Cichocki *et al.*, 2017a; Luo *et al.*, 2017; National Toxicology Program, 1977). Mice were given drinking water containing 5-bromo-2′-deoxyuridine (BrdU) 72 h prior to sacrifice. Mice were anesthetized and sacrificed by exsanguination through *vena cava* 2 h after the last dose of PCE or vehicle (n = 4–7 per group). Serum was prepared by using Z-gel tubes, and then stored at −80°C until analyzed. Tissue sections from left liver lobe and kidney were fixed in 10% formalin and embedded in paraffin. The remaining tissues were snap-frozen in liquid nitrogen and stored at −80°C until analyzed.

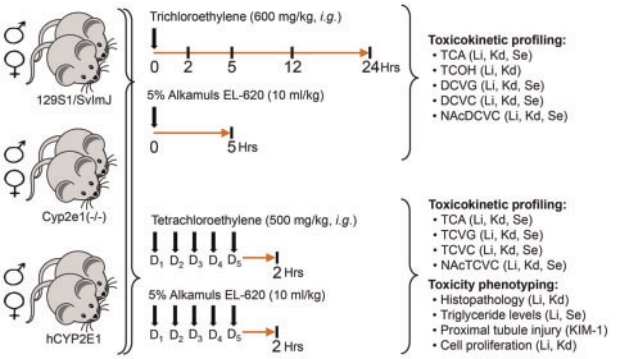

Figure 2. Schematic representation of study designs. Male and female mice from 3 strains (129S1/SvlmJ wild type, *Cyp2e1(−/−)* and *hCYP2E1*) were used in these studies. One study examined toxicokinetics of TCE in a single dose (600 mg/kg, gavage) study where samples were collected for up to 24 h. Second study examined metabolism and toxicity of PCE that was administered for 5 consecutive days (500 mg/kg, gavage); samples were collected 2 h after the last dose. Alkamuls EL-620 (5%, 10 ml/kg) was used as an aqueous emulsion vehicle for administration of both chemicals. Vertical lines indicate time points of sample collection. Down-arrows indicate chemical treatments. Endpoints collected in each study are shown as a bulleted list. Raw data for each animal and endpoint are reported in Supplementary Tables 2 and 3.

Protein measurement of CYP2E1. Total proteins were extracted from 20 mg of liver and kidney samples using T-PER Tissue Protein Extraction Reagent (Thermo Scientific, Rockford, Illinois) with Halt Protease Inhibitor Cocktail (Thermo Scientific). Protein concentration was determined using Pierce BCA Protein Assay Kit (Thermo Scientific) and a DTX 880 Multimode detector (Beckman Coulter, Brea, California). Protein extract (20 μg) was loaded onto a Mini-Protein TGX Precast Gel (Bio-Rad, Hercules, California) and transferred to a polyvinylidene difluoride membrane. Membrane was blocked with Odyssey Blocking Buffer (LI-COR, Lincoln, Nebraska), probed with CYP2E1 primary antibody (1:5000, Catalog No.: ab28146, Abcam, Cambridge, Massachusetts) or beta-actin primary antibody (1:2500, Catalog No.: ab8227, Abcam) overnight at 4°C, washed with 0.1% Tween 20 in 0.01 M PBS buffer, probed with goat anti rabbit IgG antibody (1:2500, Catalog No.: AP132P, Millipore, Billerica, Massachusetts) for 90 min at room temperature, and detected using an Odyssey Infared Imaging system (LI-COR).

Quantification of TCA. Tissue levels of TCA were measured using the US EPA method 815-B-03-002 (Domino *et al.*, 2003) with slight modifications. Tissues (50 mg) were spiked with 11 nmole of internal standard (2-bromobutyric acid), and homogenized in 1 ml of methanol:chloroform (1:1). After centrifugation at 14 000 × g for 10 min, supernatant was mixed with 1.5 ml of methanolic sulfuric acid (10%, v:v). The mixture was incubated in water batch at 55°C for 2 h to derive respective methyl esters. The derivative was then mixed well with 2 ml of methyl tert-butyl ether (MTBE) and 3 ml of sodium sulfate buffer (150 g/L). The upper layer was collected and mixed well with 3 ml of saturated

sodium bicarbonate. Again, the upper layer was collected, concentrated under nitrogen stream to a volume of approximately 20 μl, and analyzed via gas chromatography mass spectrometry. Quantitative analyses were achieved by using the peak area ratios of TCA to internal standards in an 8-point calibration curve (0, 4.1, 12.3, 37.0, 111.1, 333.3, 1000, and 3000 nmole spiked TCA).

Quantification of TCOH. Liver or kidney tissues (30 mg) were homogenized in 0.5 mL of sodium acetate (0.1 M, pH 4.6), spiked in 1000 units of beta-glucuronidase, and incubated in a thermomixer overnight at 37°C. The incubated homogenate was spiked with 20 μl of ethyl benzene (1000 nmol/ml), and then incubated in 1.5 ml of 10% sulfuric acid in methanol at 50°C for 1 h. Afterwards, the incubated solution was evenly mixed with 2 ml of MTBE and 3 ml of sodium sulfate (150 g/l), and centrifuged at 2500 × g for 3 min. The MTBE layer was neutralized by 3 mL of saturated sodium bicarbonate, collected, and concentrated with nitrogen gas to approximately 20 μl for GC-MS analysis (Song and Ho, 2003). Quantitative analyses were achieved by using the peak area ratios of TCOH to ethyl benzene in an 8-point calibration curve (0–1200 nmol TCOH/g tissue).

Quantification of D/TCVG, D/TCVC, and NAcD/TCVC. Tissue levels of dichloro and trichloro conjugates of TCE and PCE (D/TCVG, D/TCVC, and NAcD/TCVC) were evaluated as reported in (Luo *et al.*, 2017, 2018). In brief, tissue homogenate underwent a liquid-liquid extraction with 400 μl of methanol: chloroform (1:1) and a solid-phase extraction using a weak anion C-18 cartridge (Strata-X-AW, Phenomenex, Torrance, California). The eluent was dried under vacuum, and reconstituted with 50 μl of methanol:water (20:80) with 0.1% acetic acid. Tissue levels of metabolites were quantified by using the peak area ratios of standards to isotopically labeled internal standards in an 8-point calibration curve (0, 0.25, 0.5, 1.25, 2.5, 6.25, 18.75, and 31.25 pmole) via UPLC-MS/MS.

Serum alanine aminotransferase and aspartate aminotransferase. Serum alanine aminotransferase (ALT) and aspartate aminotransferase (AST) were determined by commercially available kits (Sigma Aldrich) according to the manufacturer's instructions.

Triglyceride measurements. Serum and liver triglycerides were measured with a commercially available kit (Wako, Richmond, Virginia) according to the manufacturer's instructions.

Histopathological evaluation. Formalin-fixed/paraffin embedded liver and kidney sections were stained with hematoxylin/eosin (H&E). Stained H&E slides were evaluated in a blind manner by a certificated veterinary pathologist.

KIM-1 immunohistochemistry staining. Kidney sections were dewaxed in xylene and rehydrated in graded ethanols, and then subjected to hydrochloric acid and pepsin antigen retrieval. Endogenous peroxidase activity was blocked with peroxidase and alkaline phosphatase blocking reagent (Dako, Carpinteria, California) at 25°C for 10 min. Thereafter, kidney sections were subsequently incubated with goat anti-mouse TIM-1/KIM-1/HAVCR (R&D systems, Minneapolis, Minnesota; 2 μm/ml, 10 min, room temperature) and secondary goat IgG HRP-conjugated antibody (R&D systems; 1:100, 10 min, room temperature) using Dako Antibody Dilution solution (Dako), and visualized by Dako Liquid DAB + Substrate chromogen System (Dako). Processed slides were counterstained with hematoxylin for 5 min. Quantitative analysis was performed by using Image-Pro Premier 9.1 (Media Cybernetics, Silver Spring, Maryland) at 200× magnification. Five fields of kidney section were randomly selected to calculate the percentage of positive versus total proximal tubules.

BrdU immunohistochemistry staining. Kidney sections were subject to de-paraffinization, rehydration, antigen retrieval, and peroxidase blocking procedures as described above. Thereafter, Dako EnVision System HRP kit with a monoclonal antiBrdU antibody (1:200 dilution, M074401-8, Dako) was used for detection of BrdU-incorporated nuclei. Quantitative analysis was performed by using Image-Pro Premier 9.1 (Media Cybernetics) at 200× magnification. Five fields of each kidney section were randomly selected for evaluation. Data are presented as a fraction of positively stained nuclei versus total proximal tubule nuclei (%).

RESULTS

Protein Expression of CYP2E1

CYP2E1 status in various strains was verified by genotyping before the study. In addition, to quantify the effects of treatments on CYP2E1 protein levels, we conducted Western blotting experiments. In agreement with previous studies of *Cyp2e1(−/−)* and *hCYP2E1* transgenic mice (Lu *et al.*, 2010), CYP2E1 expression in liver was higher in *hCYP2E1* mice than in Sv129 mice, it was undetectable in *Cyp2e1(−/−)* mice (Figure 3). Protein levels of CYP2E1 were much greater in liver than in kidney, also concordant with previous reports of tissue-specific differences in CYP2E1 expression in the mouse (Yue *et al.*, 2014). Low expression of CYP2E1 in mouse kidneys is also consistent with low levels of CYP2E1 in human kidneys (Fagerberg *et al.*, 2014). In addition, protein levels of CYP2E1 were slightly higher in liver of male mice as compared with female mice. This sex-dependent difference was even more pronounced in kidneys where no detectable CYP2E1 protein was found in females. The sex difference was not observed in the liver of Sv129 mice (Nakajima *et al.*, 2000) or CD-1 mice (Hoivik *et al.*, 1995); however, it was observed in kidney of CD-1 mice (Hoivik, et al., 1995) where protein level of CYP2E1 was higher in male mice as compared with female mice. We found that TCE induced expression in CYP2E1 only in liver of female mice of both *hCYP2E1* and Sv129 strains, suggesting that TCE treatment and sex hormones may regulate liver expression of CYP2E1.

The Role of CYP2E1 in Toxicokinetics of TCE

We sought to examine TCE toxicokinetics as a factor of CYP2E1 status in each strain and sex. We examined concentration-time profiles of TCA, TCOH, DCVG and NAcDCVC in liver (Figure 4). In male Sv129 mice, we found that liver toxicokinetics of TCA, TCOH, and DCVG were similar to those reported in previous studies using 129S1/SvImJ mice (Yoo *et al.*, 2015a,c), B6C3F1/J mice (Luo *et al.*, 2018), and Collaborative Cross mice (Venkatratnam *et al.*, 2017). The area under curve (AUC) analysis of the metabolite levels revealed sex-dependent differences in liver toxicokinetics of TCE. In Sv129 mice, AUC was higher in male mice as compared with female mice for TCA and TCOH (2.2-fold for TCA and 33.9-fold for TCOH), but lower for DCVG and NAcDCVC(1.9-fold for DCVG and 1.6-fold for NacDCVC). The sex-dependent differences in liver toxicokinetics for TCA and TCOH were also observed in the previous study (Yoo *et al.*, 2015c), whereas the sex differences for liver toxicokinetics of DCVG and NAcDCVC have not been previously investigated.

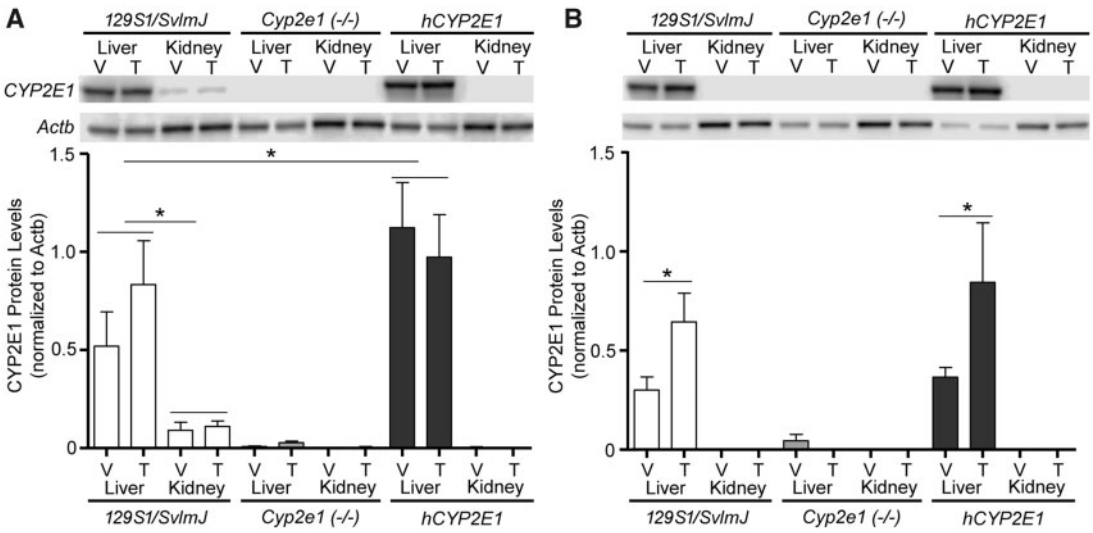

Figure 3. Protein expression of CYP2E1 in liver and kidney of (A) male and (B) female 129S1/SvlmJ, *Cyp2e1(−/−)*, and *hCYP2E1* mice at 4 hours after dosing with a single dose of vehicle (V, Alkamuls EL-620) or TCE (T, 600 mg/kg). Representative Western blots and quantitative analysis of CYP2E1 protein expression are shown ($n = 4$/group). Expression of beta actin (Actb) was used to normalize for protein loading. Data are shown as mean ± SD. Asterisks denote statistical significant difference between groups (1-way ANOVA with Newman-Keuls *post hoc* test, $p < .05$).

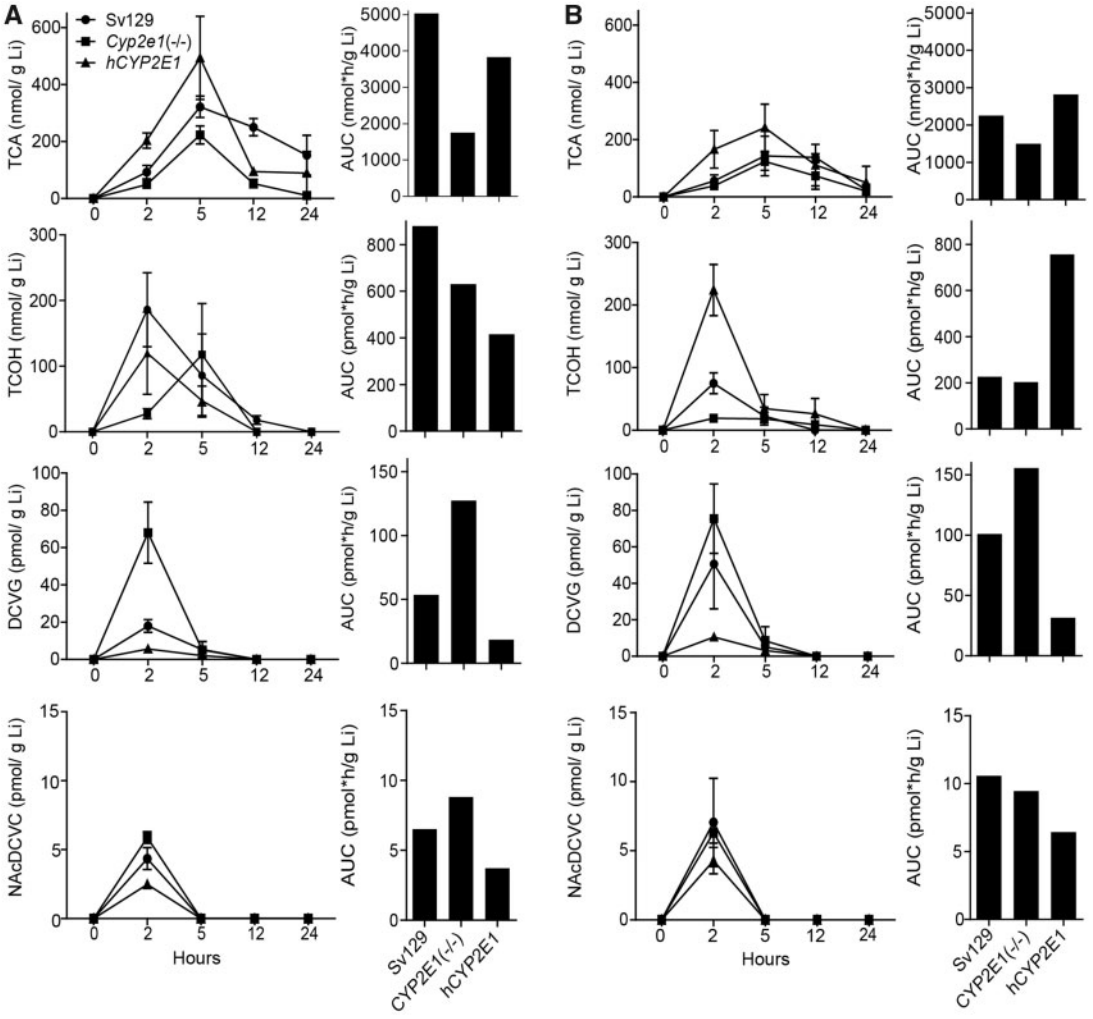

Figure 4. Comparative analysis of liver (Li) toxicokinetics of major oxidative (TCA and TCOH), and GSH conjugation (DCVG) metabolites of TCE (600 mg/kg) in (A) male and (B) female 129S1/SvlmJ *(SV129)*, *Cyp2e1(−/−)*, and *hCYP2E1* mice. Average kinetic profiles (left panels, strains are identified by symbols as shown in an inset in the top left graph) and AUC (right panels) are shown ($n = 2$–4 per group per time point, as detailed in Supplementary Table 2).

In agreement with the lack of CYP2E1 expression, the AUCs were 2.9-fold lower for TCA, and 1.4-fold lower for TCOH in male *Cyp2e1(−/−)* mice as compared with those in male Sv129 mice. A decrease in formation of oxidative metabolites of TCE was less pronounced in female *Cyp2e1(−/−)* mice. Interestingly, elimination of TCA in the liver was slower in Sv129 mice as compared with *Cyp2e1(−/−)* and *hCYP2E1* mice. Slower formation of TCOH was most pronounced in male *Cyp2e1(−/−)* mice with a peak concentration (C_{max}) at 5 h and the differences in the timing of C_{max} for TCOH between *Cyp2e1(−/−)*and *hCYP2E1* mice may have affected the AUC values. Interestingly, the AUC of DCVG was 1.5- to 2.4-fold higher in *Cyp2e1(−/−)* mice of both sexes, but 2.9- to 3.2-fold lower in *hCYP2E1* mice as compared with Sv129 mice. For the AUCs of NAcTCVC, similar trend was observed in male mice but not in female mice.

Metabolites from GSH conjugative pathway have been postulated to cause kidney toxicity; therefore, we also examined concentration-time profiles of TCA, DCVG, DCVC, and NAcDCVC in the kidney (Figure 5). In male Sv129 mice, we found that kidney toxicokinetics of TCA, DCVG, and DCVC was similar to that previously reported in 129S1/SvImJ mice (Yoo *et al.*, 2015c), B6C3F1/J mice (Luo *et al.*, 2018), and C57BL/6J and NOD/ShiLtJ mice (Yoo *et al.*, 2015b). Similar to the observations in the liver, there were pronounced sex-dependent differences in kidney levels of TCA, TCOH (Supplementary Table 4), and NAcDCVC. In male Sv129 mice, the kidney AUC values were 2.2-fold higher for TCA, but 2.5-fold lower for NAcDCVC compared with female mice. With respect to the CYP2E1-mediated effects, the kidney AUCs were 1.6- to 5.1-fold lower for TCA, and 1.9- to 3.3-fold lower for TCOH in *Cyp2e1(−/−)* mice as compared with Sv129 mice, whereas these differences were less pronounced in female mice. Interestingly, in both male and female mice, the elimination of TCA was the slowest in the kidney of Sv129 of the strains examined herein. The AUC of DCVG was 1.4- to 1.9-fold higher in *Cyp2e1(−/−)* mice, but 1.2- to 1.4-fold lower in *hCYP2E1* mice, as compared with Sv129 mice.

Comparison of the Effect of CYP2E1 on Metabolisms of TCE and PCE

Much less is known about metabolism and toxicity of PCE, as compared with TCE (Cichocki *et al.*, 2016). No study has tested the role of CYP2E1 in metabolism of PCE. Therefore, we compared the levels of key oxidative and GSH conjugation metabolites of TCE and PCE in the liver and kidney of 3 strains of mice 2 h after the last dose (Figure 6). The comparison for TCA levels between TCE-treated and PCE-treated mice has limitations because TCE was administered as a single dose while PCE treatment was repeated over 5 days; still, the patterns of differences between sexes and strains are informative. In Sv129 strain, liver levels of TCA were about 2-fold higher in PCE-treated male and female mice as compared with TCE-treated mice. In our recent study in B6C3F1 mice we found that at equimolar doses, more TCA was found in both liver and kidney tissue from PCE-exposed mice compared with TCE-exposed groups (Zhou *et al.*, 2017). In male and female *Cyp2e1(−/−)* mice, TCA level in liver was about half of that in Sv129 mice. At the same time, TCA levels in liver of *hCYP2E1* mice were the same as in Sv129 mice, in both males and females.

Importantly, there are major differences in the flux of metabolism through GSH pathway for PCE as compared with TCE, even though we consider different dosing designs between TCE and PCE. Metabolites from GSH conjugative pathway are rapidly excreted within 24 h after dosing. In addition, the relationship between T/PCE dose and GSH metabolites is linear within the dose range used in this study. Therefore, the comparison for GSH conjugates between TCE and PCE is more relevant than that for TCA levels. In the liver, the GSH conjugate of PCE—TCVG—was found to be present at over 5-fold greater levels than DCVG. Kidney GSH metabolites of PCE—TCVC and NAcTCVC—were found in the amounts greater than one order of magnitude than DCVC and NAcDCVC. Interestingly, levels of TCVG in the liver and TCVC in the kidney were lower in male *Cyp2e1(−/−)* mice, but unchanged in female *Cyp2e1(−/−)* mice. NAcTCVC in the kidney was lower in male and female *Cyp2e1(−/−)* mice as compared with either Sv129 or *hCYP2E1* mice.

Effect of CYP2E1 on PCE-Induced Liver and Kidney Toxicity

We also examined whether strain-specific differences in PCE metabolism are associated with differences in toxicity in liver and kidney. Liver toxicity was investigated by histopathological evaluation, triglycerides measurements, and assessment of cell proliferation. Treatment with PCE for 5 days induced lipid accumulation in the liver of male Sv129 mice, but had no such effect in male *Cyp2e1(−/−)* or *hCYP2E1* mice (Figure 7A). This histopathological finding was confirmed by measurements of liver and serum triglycerides. Liver triglycerides were about 6-fold higher and serum about 2-fold lower in PCE-treated male Sv129 mice as compared with vehicle-treated mice (Figs. 7B and 7C). Similar observations were made in female mice of 3 strains, with PCE effect being observed only in Sv129 mice (raw data are available in Supplementary Table 3). There was no PCE-induced acute liver injury as assessed by serum ASTs and ALT, and there was no significant effect on liver cell proliferation (Supplementary Table 3).

Kidney effects of PCE were evaluated by measuring proximal tubule injury and cell proliferation in male (Figure 8) and female mice (Supplementary Table 3). We found that PCE treatment induced proximal tubule injury (16.4%–39.3% increase in KIM-1 positive proximal tubules), an effect that was significant in male and female Sv129 mice and male *hCYP2E1* mice. No increase in cell proliferation was found in the kidney of PCE-treated male mice; in fact, cell proliferation was lower in PCE-treated male Sv129 mice compared with strain-matched control group. Interestingly, we found higher basal levels of proximal tubule injury and cell proliferation in kidneys of female mice as compared with male mice (Supplementary Table 3).

DISCUSSION

The role of CYP2E1 in TCE metabolism has been studied by comparing wild-type mice and CYP2E1 transgenic mice (Forkert *et al.*, 2006; Kim and Ghanayem, 2006; Ramdhan, et al., 2008). Even though these studies focused on CYP2E1-mediated toxic effects of TCE, CYP2E1-mediated effects on metabolism were also investigated by measuring the urinary excretion of TCA and TCOH. Decreased TCA and TCOH levels were found in urine of *Cyp2e1(−/−)* mice; however, the internal dosimetry of these oxidative metabolites in liver and kidney, as well as that of GSH conjugation metabolites, was not explored in these studies. To address this significant data gap, we conducted a study of concentration-time profiles of both oxidative and GSH conjugation metabolites of TCE in liver and kidney. Furthermore, we included both *Cyp2e1(−/−)* and *hCYP2E1* mice and both males and females to provide insights into the role that CYP2E1 plays in TCE metabolism. We also extended this study to investigate the CYP2E1-mediated metabolism and toxic effects of a related chemical of human health concern, PCE.

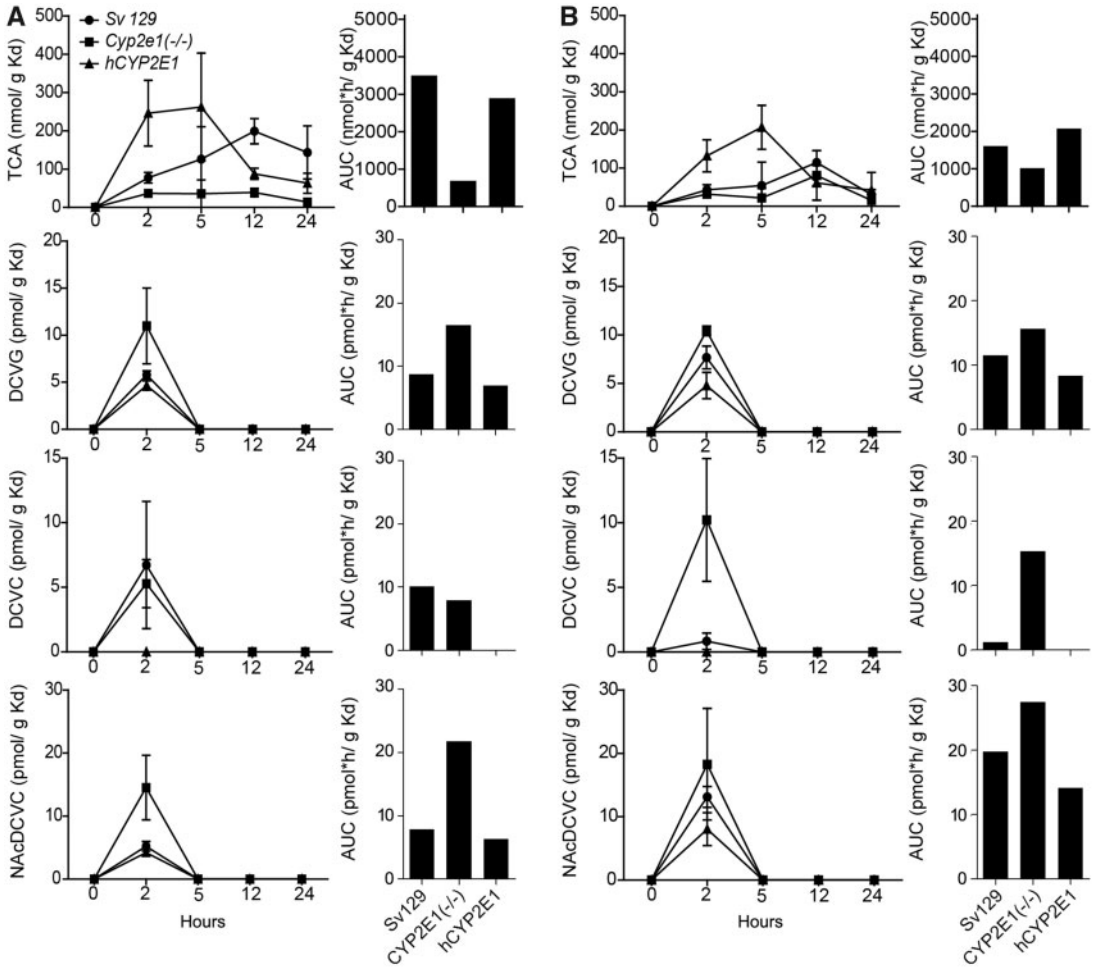

Figure 5. Comparative analysis of kidney (Kd) toxicokinetics of oxidative (TCA), and GSH conjugation metabolites (DCVG, DCVC, and NAcDCVC) of TCE (single dose, 600 mg/kg) in (A) male and (B) female 129S1/SvlmJ (*SV129*), *Cyp2e1(−/−)*, and *hCYP2E1* mice. Average kinetic profiles (left panels, strains are identified by symbols as shown in an inset in the top left graph) and AUC (right panels) are shown ($n = 2$–4 per group per time point, as detailed in Supplementary Table 2).

First, we found that CYP2E1 plays a role in generation of oxidative metabolites of TCE in liver and kidney. Formation of TCA from TCE in liver was reduced by about 65% without the expression of CYP2E1, which concurs with previous observations in urine of *Cyp2e1(−/−)* mice (Ramdhan *et al.*, 2008). However, *Cyp2e1(−/−)* mice still can generate TCA from TCE, suggesting that other CYPs, such as CYP2F and CYP2B1, may also participate in TCE oxidation (Forkert *et al.*, 2005). Interestingly, *Cyp2e1(−/−)* mice exhibit a retarded T_{max} for TCOH, but generate a comparable amount of TCOH in liver. In addition, *hCYP2E1* mice, which had the highest level of CYP2E1 expression in liver, formed the lowest amount of TCOH. Collectively, these results suggest that CYP2E1 plays a major, but not exclusive, role in converting TCOH to TCA. Importantly, in absence of CYP2E1 expression, an increase in generation of GSH conjugates was observed. This result supports the notion that even though GSH conjugation is a minor pathway of TCE metabolism in the mouse, CYP-mediated oxidation does compete with GSH conjugation.

Second, we observed differences in the extent of metabolism between TCE and PCE, and that CYP2E1 also has a role in formation of TCA in PCE-treated mice. It has been assumed that PCE metabolism and toxicity are similar to TCE due to their structural similarity (Cichocki *et al.*, 2016). Even though qualitative and quantitative differences in oxidative metabolisms between TCE and PCE are known (IARC, 2014; U.S. EPA, 2011a,b), data on GSH conjugation metabolism are still limited. Overall, the flux to both oxidative and GSH conjugation metabolites is higher in PCE-treated mice compared with TCE-treated mice. Taking into account the dose differences, we found that PCE-produced metabolite levels were approximately 3-fold greater for TCA, 4-fold greater for the GSH conjugate, and 25-fold greater for cysteine and n-acetyl cysteine conjugates. These quantitative differences are in agreement with those reported recently (Luo *et al.*, 2017, 2018; Zhou *et al.*, 2017).

In addition, our results show that CYP2E1 status could modify GSH conjugative metabolism differently between TCE and PCE. Knocking out the expression of CYP2E1 led to increases in DCVG, DCVC, and NAcDCVC, but decreases levels of TCVG, TCVC, and NAcTCVC in livers and kidneys. In PCE-treated mice, CYP2E1-mediated oxidation was not competing with the GSH conjugation. This suggests that other CYPs could be important in PCE oxidation. An *in vitro* study also showed that PCE oxidation is primarily catalyzed by the CYP2B family, rather than CYP2E1 (White and De Matteis, 2001). The role for CYP2E1 in the conversion from TCOH to TCA may also account for, at least in part, the competition between oxidation and GSH conjugation pathways in TCE-treated mice. TCOH is a TCE-specific

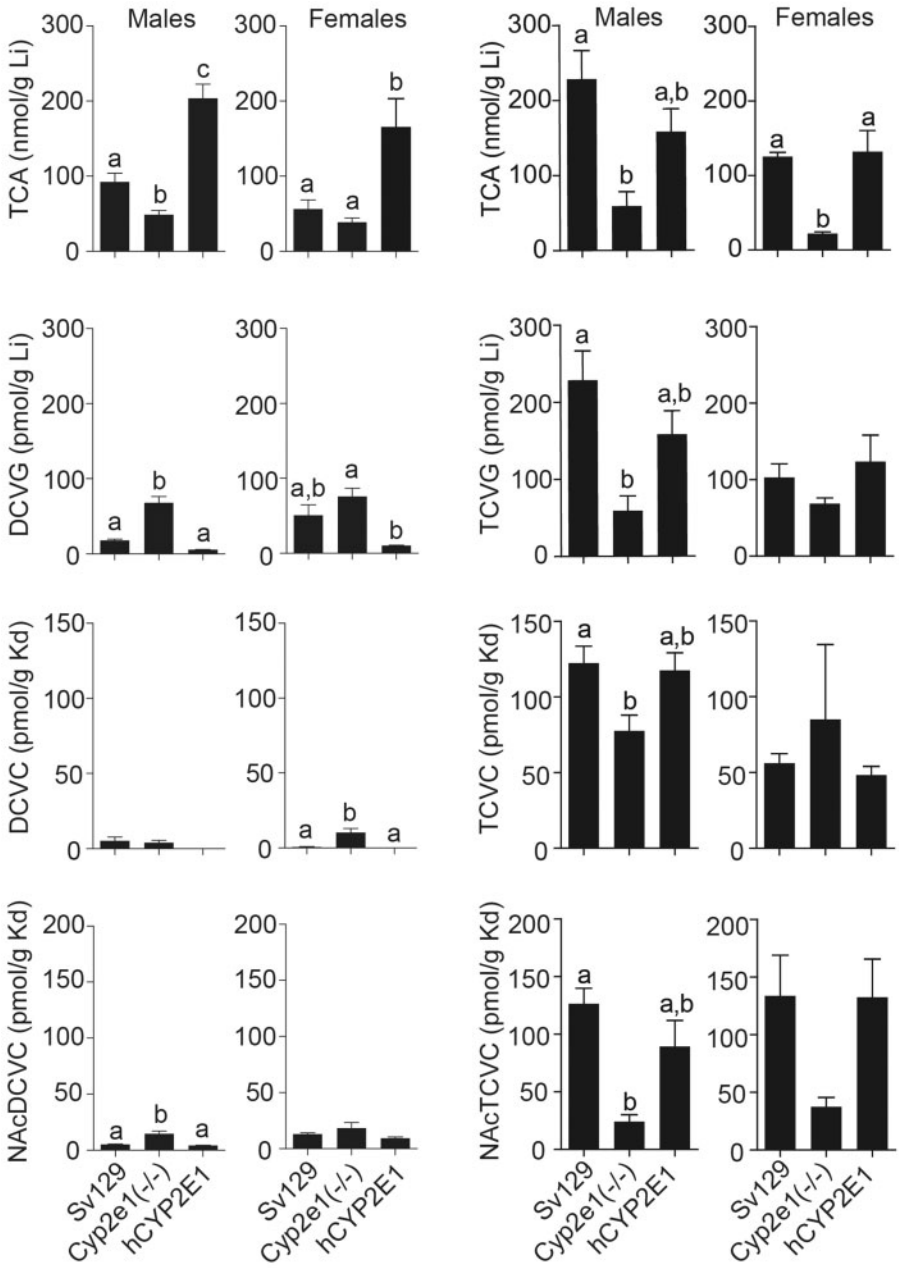

Figure 6. Comparative analysis of liver (Li) and kidney (Kd) levels of major oxidative (TCA), and GSH conjugation (DCVG, DCVC, and NAcDCVC for TCE; TCVG, TCVC, and NAcTCVC for PCE) metabolites. Data for (A) TCE (600 mg/kg) and (B) PCE (5 daily doses, 500 mg/kg) in male and female 129S1/SvlmJ (Sv129), *Cyp2e1*(−/−), and *hCYP2E1* mice are shown. Metabolite levels shown are for a 2 h time point after dosing. Data are shown as mean ± SD. Bars with different letters are significantly different (1-way ANOVA with Newman-Keuls post hoc test, $p < .05$).

metabolite (Chiu *et al.*, 2007; Zhou, et al., 2017) and the conversion from TCOH to TCA is thought to be catalyzed by CYPs (Lash *et al.*, 2014). Lack of CYP2E1 was likely the cause of TCOH accumulation, which in turn impedes the initial oxidation of TCE. Correspondingly, the total flux through GSH conjugation would increase in CYP-deficient individuals.

Third, we found that presence of mouse CYP2E1 results in PCE-induced liver steatosis, while kidney effects of PCE are largely unaffected by CYP2E1 status. Liver fat accumulation has been reported in PCE-treated mice but not in TCE-treated mice (Buben and O'Flaherty, 1985; Cichocki *et al.*, 2017b). However, liver steatosis was observed in TCE-treated, *Pparα*(−/−) and *hPPARα* transgenic mice (Ramdhan *et al.*, 2010). PPARα activation results in an increase in fatty acid catabolism in liver (Rakhshandehroo *et al.*, 2010; Ramdhan, et al., 2010), and the suppression of PPARα activation causes hepatosteatosis. Interestingly, hepatic level of TCA, a PPARα activator, was the highest in liver of wild type mice compared with *Pparα*(−/−) and *hPPARα* transgenic mice (Yoo *et al.*, 2015c), supporting the aforementioned hypothesis. In our study, the amount of TCA generated in PCE-treated mice was even greater than that in TCE-treated mice; however, we found fat accumulation in the liver of Sv129 mice. Surprisingly, there was no liver steatosis in PCE-treated *Cyp2e1*(−/−) and *hCYP2E1* mice. These observations suggest that, aside from PPARα activation, CYP2E1 status also may affect lipid metabolism in liver. Additional studies are

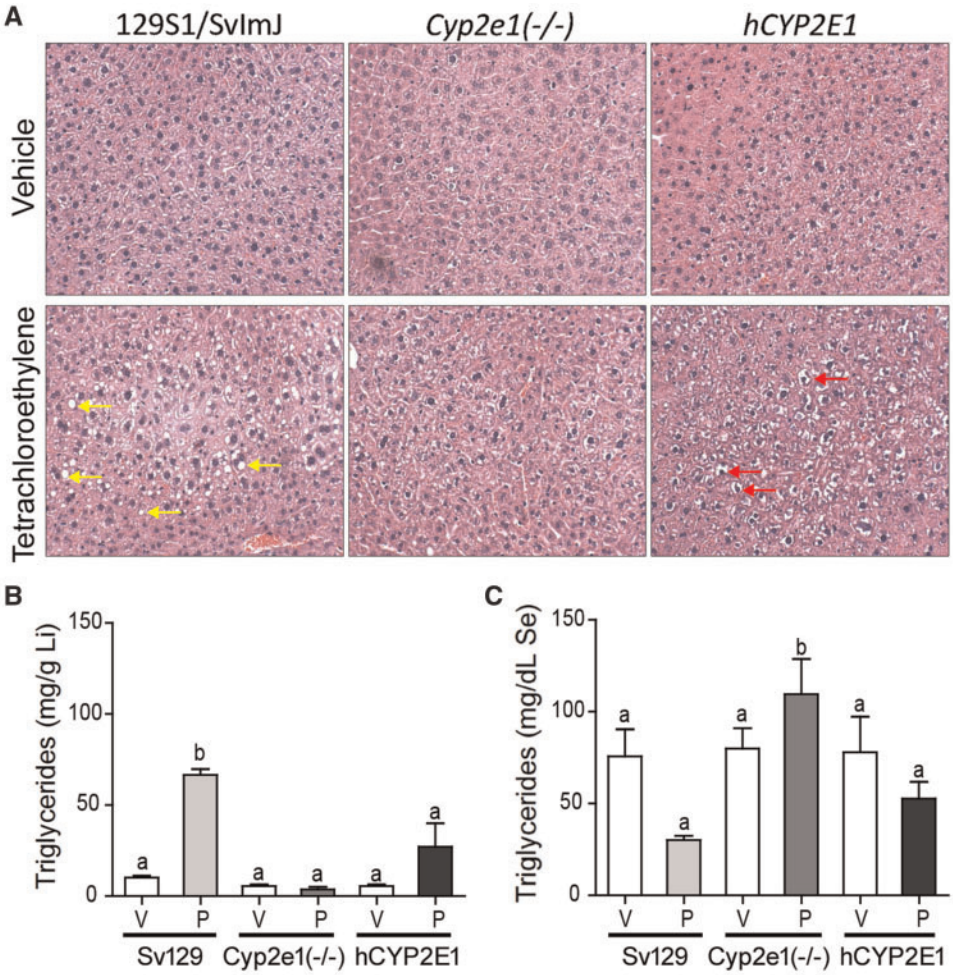

Figure 7. Effects of PCE on liver fat accumulation in male 129S1/SvImJ (*Sv129*), *Cyp2e1*(−/−), and *hCYP2E1* mice treated with 5 consecutive daily doses of vehicle (V, Alkamuls EL-620) or PCE (P, 500 mg/kg). (A) Representative images of H&E staining with 200× magnification. Arrows point to fat accumulation in Sv129 mice and glycogen accumulation in hCYP2E1 mice. Triglyceride levels in (B) liver (Li) and (C) serum (Se) are shown as mean ± SD. Bars with letters are significantly different from other groups (1-way ANOVA with Newman-Keuls *post hoc* test, $p < .05$).

required to uncover the underlying molecular mechanisms behind the CYP2E1-mediated effects of PCE in mouse liver.

Similar to no effect of CYP2E1 status on GSH conjugation metabolite formation from PCE, we found no effect of CYP2E1 status on kidney injury. We did observe an increase in KIM-1 staining in PCE-treated mice, showing that kidney is a target tissue in the mouse. It has been postulated that the bio-activation of TCVC and NAcTCVC, catalyzed by renal β lyase or other enzymes such as flavin monooxygenase and CYP3A, is a critical step for nephrotoxicity of PCE (Irving *et al.*, 2013; Lash *et al.*, 1994). It is likely that CYP2E1 may also play a role in sulfoxidation of cysteine and n-acetyl cysteine conjugates of PCE, as it was shown that CYP2E1 is involved in sulfoxidation of S-methyl N, N-diethylthiolcarbamate (Madan *et al.*, 1995) and diethyldithiocarbamate methyl ester (Madan *et al.*, 1998).

Fourth, our data provide important clues into sex differences in metabolism and toxicity of chlorinated solvents. Protein levels of CYP2E1, as well as the oxidative metabolites of TCE and PCE, were higher in liver and kidney of male mice as compared with female mice. The sex-dependent difference in metabolism of TCE was previously reported (Yoo *et al.*, 2015c). Indeed, studies showed that steroid sex hormones can regulate constitutive expression of CYP2E1 in mice (Konstandi *et al.*, 2013; Penaloza *et al.*, 2014), which can further modulate chemical-induced toxicity (Hu *et al.*, 1993).

We also note that this study is not without limitations. First, the experimental designs were not identical between TCE and PCE arms of the study. Still, we are able to indirectly compare TCE and PCE metabolites, and we report that there are potential differences in GSH conjugative metabolism between TCE and PCE. However, a direct comparison between toxicokinetics of TCE and PCE will further advance our knowledge in the relationship between metabolism and toxicity. Second, due to difficulties in breeding transgenic mice, the number of *Cyp2e1*(−/−) mice were limited. Future studies may benefit from increasing the sample size and breeding scale, if technically and economically possible.

In summary, this study provides a comprehensive analysis of the role of CYP2E1 in the metabolism and toxicity of TCE and PCE. CYP2E1 status affects levels of both oxidative and GSH conjugation metabolites in mouse liver and kidney. We conclude that CYP2E1 is an important, but not exclusive actor in the oxidative metabolism and toxicity of TCE and PCE. CYP2E1 status also affects liver fat accumulation in PCE-treated mice.

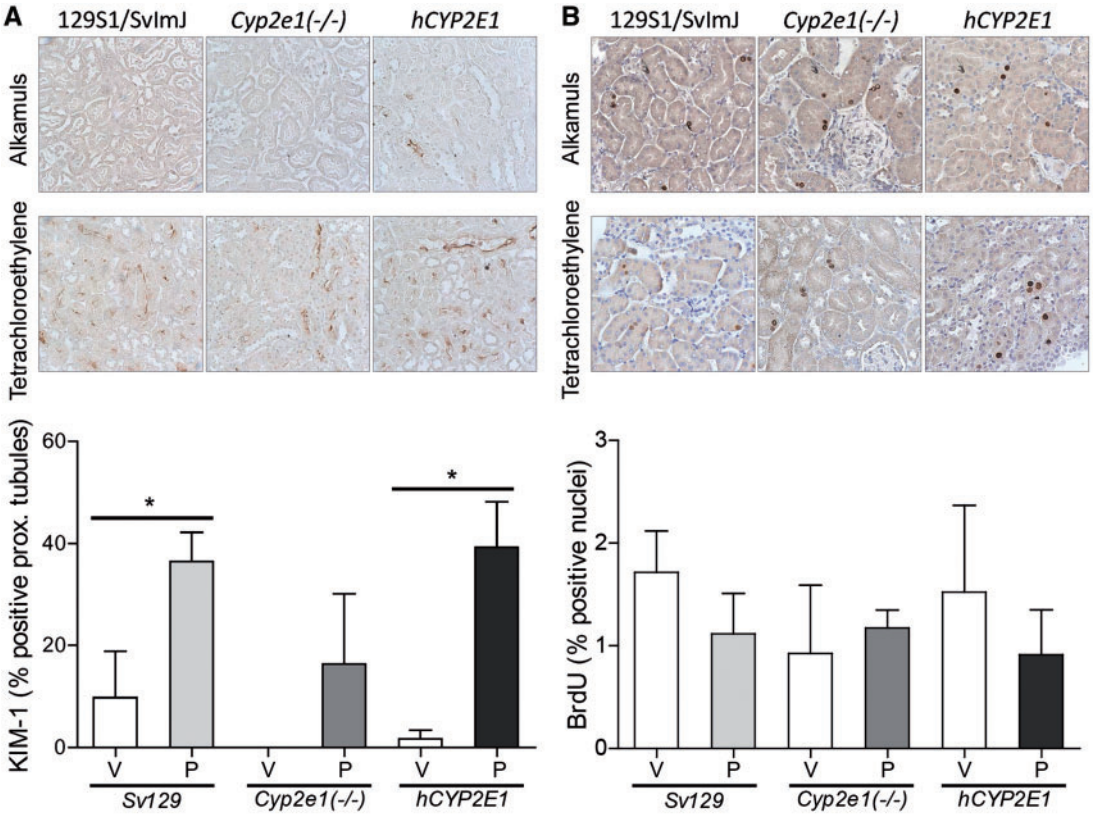

Figure 8. Effects of PCE on (A) proximal tubule injury and (B) cell proliferation in kidney of male 129S1/SvImJ (*SV129*), *Cyp2e1* (−/−), and *hCYP2E1* mice treated with 5 consecutive daily doses of vehicle (V, Alkamuls EL-620) or PCE (P, 500 mg/kg). The top figures show the representative images of KIM-1 or BrdU staining with 400× magnification. Quantitative results of proximal tubule injury and cell proliferation are expressed as % positive/total proximal tubules or nuclei, and are summarized in the lower bar charts. Asterisks denote significant difference by paired t test ($p < .05$).

SUPPLEMENTARY DATA

Supplementary data are available at *Toxicological Sciences* online.

ACKNOWLEDGMENTS

The authors wish to thank Dr Anthony H. Knap, Dr Terry Wade, Dr Stephen Sweet, and Dr Thomas J. McDonald at Texas A&M University for technical support. The authors also thank Dr Joseph A. Cichocki and Mr Abhishek Venkatratnam for the fruitful discussions of the study design.

FUNDING

This work was supported by grants from the National Institutes of Health [grant number P42 ES005948] and the United States Environmental Protection Agency [grant number STAR RD83561202].

REFERENCES

Agency for Toxic Substances and Disease Registry (ATSDR). 2014. Draft Toxicological Profile for Tetrachloroethylene. U.S. Department of Health and Human Services, Public Health Service. Atlanta, GA.

Buben, J. A., and O'Flaherty, E. J. (1985). Delineation of the role of metabolism in the hepatotoxicity of trichloroethylene and perchloroethylene: A dose-effect study. *Toxicol. Appl. Pharmacol.* **78**, 105–122.

Chiu, W. A., Micallef, S., Monster, A. C., and Bois, F. Y. (2007). Toxicokinetics of inhaled trichloroethylene and tetrachloroethylene in humans at 1 ppm: Empirical results and comparisons with previous studies. *Toxicol. Sci.* **95**, 23–36.

Chiu, W. A., Okino, M. S., and Evans, M. V. (2009). Characterizing uncertainty and population variability in the toxicokinetics of trichloroethylene and metabolites in mice, rats, and humans using an updated database, physiologically based pharmacokinetic (PBPK) model, and Bayesian approach. *Toxicol. Appl. Pharmacol.* **241**, 36–60.

Cichocki, J. A., Furuya, S., Konganti, K., Luo, Y. S., McDonald, T. J., Iwata, Y., Chiu, W. A., Threadgill, D. W., Pogribny, I. P., and Rusyn, I. (2017). Impact of nonalcoholic fatty liver disease on toxicokinetics of tetrachloroethylene in mice. *J. Pharmacol. Exp. Ther.* **361**, 17–28.

Cichocki, J. A., Furuya, S., Venkatratnam, A., McDonald, T. J., Knap, A. H., Wade, T., Sweet, S., Chiu, W. A., Threadgill, D. W., and Rusyn, I. (2017). Characterization of variability in toxicokinetics and toxicodynamics of tetrachloroethylene using the collaborative cross mouse population. *Environ. Health Perspect.* **125**, 057006.

Cichocki, J. A., Guyton, K. Z., Guha, N., Chiu, W. A., Rusyn, I., and Lash, L. H. (2016). Target organ metabolism, toxicity, and mechanisms of trichloroethylene and perchloroethylene: Key similarities, differences, and data gaps. *J. Pharmacol. Exp. Ther.* **359**, 110–123.

Domino, M. M., Pepich, B. V., Munch, D. J., Fair, P. S., and Xie, Y. (2003). Method 552.3: Determination of haloacetic acids and dalapon in drinking water by liquid-liquid microextraction,

derivatization, and gas chromatography with electron capture detection. Office of Ground Water and Drinking Water, Cincinnati, OH.

Elfarra, A. A., and Krause, R. J. (2007). S-(1, 2, 2-trichlorovinyl)-L-cysteine sulfoxide, a reactive metabolite of S-(1, 2, 2-Trichlorovinyl)-L-cysteine formed in rat liver and kidney microsomes, is a potent nephrotoxicant. *J. Pharmacol. Exp. Ther.* **321**, 1095–1101.

Fagerberg, L., Hallström, B. M., Oksvold, P., Kampf, C., Djureinovic, D., Odeberg, J., Habuka, M., Tahmasebpoor, S., Danielsson, A., Edlund, K., *et al.* (2014). Analysis of the human tissue-specific expression by genome-wide integration of transcriptomics and antibody-based proteomics. *Mol. Cell Proteomics* **13**, 397–406.

Forkert, P. G., Baldwin, R. M., Millen, B., Lash, L. H., Putt, D. A., Shultz, M. A., and Collins, K. S. (2005). Pulmonary bioactivation of trichloroethylene to chloral hydrate: Relative contributions of CYP2E1, CYP2F, and CYP2B1. *Drug Metab. Dispos.* **33**, 1429–1437.

Forkert, P. G., Millen, B., Lash, L. H., Putt, D. A., and Ghanayem, B. I. (2006). Pulmonary bronchiolar cytotoxicity and formation of dichloroacetyl lysine protein adducts in mice treated with trichloroethylene. *J Pharmacol. Exp. Ther.* **316**, 520–529.

Guha, N., Loomis, D., Grosse, Y., Lauby-Secretan, B., El Ghissassi, F., Bouvard, V., Benbrahim-Tallaa, L., Baan, R., Mattock, H., and Straif, K. (2012). Carcinogenicity of trichloroethylene, tetrachloroethylene, some other chlorinated solvents, and their metabolites. *Lancet Oncol.* **13**, 1192–1193.

Hanioka, N., Jinno, H., Takahashi, A., Nakano, K., Yoda, R., Nishimura, T., and Ando, M. (1995). Interaction of tetrachloroethylene with rat hepatic microsomal P450-dependent monooxygenases. *Xenobiotica* **25**, 151–165.

Hoivik, D. J., Manautou, J. E., Tveit, A., Hart, S. G., Khairallah, E. A., and Cohen, S. D. (1995). Gender-related differences in susceptibility to acetaminophen-induced protein arylation and nephrotoxicity in the CD-1 mouse. *Toxicol. Appl. Pharmacol.* **130**, 257–271.

Hu, J. J., Lee, M. J., Vapiwala, M., Reuhl, K., Thomas, P. E., and Yang, C. S. (1993). Sex-related differences in mouse renal metabolism and toxicity of acetaminophen. *Toxicol. Appl. Pharmacol.* **122**, 16–26.

IARC. (2014). Trichloroethylene, tetrachloroethylene and some other chlorinated agents. *IARC Monogr. Eval Carcinog. Risks Hum.* **106**, 35–329.

Irving, R. M., Pinkerton, M. E., and Elfarra, A. A. (2013). Characterization of the chemical reactivity and nephrotoxicity of N-acetyl-S-(1, 2-dichlorovinyl)-L-cysteine sulfoxide, a potential reactive metabolite of trichloroethylene. *Toxicol. Appl. Pharmacol.* **267**, 1–10.

Jia, C., Yu, X., and Masiak, W. (2012). Blood/air distribution of volatile organic compounds (VOCs) in a nationally representative sample. *Sci. Total Environ.* **419**, 225–232.

Kim, D., and Ghanayem, B. I. (2006). Comparative metabolism and disposition of trichloroethylene in Cyp2e1-/-and wild-type mice. *Drug Metab. Dispos.* **34**, 2020–2027.

Konstandi, M., Cheng, J., and Gonzalez, F. J. (2013). Sex steroid hormones regulate constitutive expression of Cyp2e1 in female mouse liver. *Am. J. Physiol. Endocrinol. Metab.* **304**, E1118–E1128.

Lash, L. H., Chiu, W. A., Guyton, K. Z., and Rusyn, I. (2014). Trichloroethylene biotransformation and its role in mutagenicity, carcinogenicity and target organ toxicity. *Mutat. Res. Rev. Mutat. Res.* **762**, 22–36.

Lash, L. H., Fisher, J. W., Lipscomb, J. C., and Parker, J. C. (2000). Metabolism of trichloroethylene. *Environ. Health Perspect.* **108(Suppl 2)**, 177–200.

Lash, L. H., Hueni, S. E., and Putt, D. A. (2001). Apoptosis, necrosis, and cell proliferation induced by S-(1, 2-dichlorovinyl)-L-cysteine in primary cultures of human proximal tubular cells. *Toxicol. Appl. Pharmacol.* **177**, 1–16.

Lash, L. H., Putt, D. A., Hueni, S. E., Krause, R. J., and Elfarra, A. A. (2003). Roles of necrosis, Apoptosis, and mitochondrial dysfunction in S-(1, 2-dichlorovinyl)-L-cysteine sulfoxide-induced cytotoxicity in primary cultures of human renal proximal tubular cells. *J. Pharmacol. Exp. Ther.* **305**, 1163–1172.

Lash, L. H., Sausen, P. J., Duescher, R. J., Cooley, A. J., and Elfarra, A. A. (1994). Roles of cysteine conjugate beta-lyase and S-oxidase in nephrotoxicity: Studies with S-(1, 2-dichlorovinyl)-L-cysteine and S-(1, 2-dichlorovinyl)-L-cysteine sulfoxide. *J. Pharmacol. Exp. Ther.* **269**, 374–383.

Laughter, A. R., Dunn, C. S., Swanson, C. L., Howroyd, P., Cattley, R. C., and Corton, J. C. (2004). Role of the peroxisome proliferator-activated receptor alpha (PPARalpha) in responses to trichloroethylene and metabolites, trichloroacetate and dichloroacetate in mouse liver. *Toxicology* **203**, 83–98.

Lin, J. H., and Lu, A. Y. (2001). Interindividual variability in inhibition and induction of cytochrome P450 enzymes. *Annu. Rev. Pharmacol. Toxicol.* **41**, 535–567.

Lu, Y., Wu, D., Wang, X., Ward, S. C., and Cederbaum, A. I. (2010). Chronic alcohol-induced liver injury and oxidant stress are decreased in cytochrome P4502E1 knockout mice and restored in humanized cytochrome P4502E1 knock-in mice. *Free Radic. Biol. Med.* **49**, 1406–1416.

Luo, Y. S., Cichocki, J. A., McDonald, T. J., and Rusyn, I. (2017). Simultaneous detection of the tetrachloroethylene metabolites S-(1, 2, 2-trichlorovinyl) glutathione, S-(1, 2, 2-trichlorovinyl)-L-cysteine, and N-acetyl-S-(1, 2, 2-trichlorovinyl)-L-cysteine in multiple mouse tissues via ultra-high performance liquid chromatography electrospray ionization tandem mass spectrometry. *J. Toxicol. Environ. Health A* **80**, 513–524.

Luo, Y. S., Furuya, S., Chiu, W., and Rusyn, I. (2018). Characterization of inter-tissue and inter-strain variability of TCE glutathione conjugation metabolites DCVG, DCVC, and NAcDCVC in the mouse. *J. Toxicol. Environ. Health A* **81**, 37–52.

Madan, A., Parkinson, A., and Faiman, M. D. (1995). Identification of the human and rat P450 enzymes responsible for the sulfoxidation of S-methyl N, N-diethylthiolcarbamate (DETC-ME). The terminal step in the bioactivation of disulfiram. *Drug Metab. Dispos.* **23**, 1153–1162.

Madan, A., Parkinson, A., and Faiman, M. D. (1998). Identification of the human P-450 enzymes responsible for the sulfoxidation and thiono-oxidation of diethyldithiocarbamate methyl ester: Role of P-450 enzymes in disulfiram bioactivation. *Alcohol Clin. Exp. Res.* **22**, 1212–1219.

Nakajima, T., Kamijo, Y., Usuda, N., Liang, Y., Fukushima, Y., Kametani, K., Gonzalez, F. J., and Aoyama, T. (2000). Sex-dependent regulation of hepatic peroxisome proliferation in mice by trichloroethylene via peroxisome proliferator-activated receptor alpha (PPARalpha). *Carcinogenesis* **21**, 677–682.

Nakajima, T., Wang, R. S., Elovaara, E., Park, S. S., Gelboin, H. V., and Vainio, H. (1993). Cytochrome P450-related differences between rats and mice in the metabolism of benzene, toluene and trichloroethylene in liver microsomes. *Biochem. Pharmacol.* **45**, 1079–1085.

National Toxicology Program. (1977). Bioassay of tetrachloroethylene for possible carcinogenicity. *Natl. Cancer Inst. Carcinog. Tech. Rep. Ser.* **13**, 1–83.

National Toxicology Program. (1990). Carcinogenesis Studies of Trichloroethylene (Without Epichlorohydrin) (CAS No. 79-01-6) in F344/N Rats and B6C3F1 Mice (Gavage Studies). *Natl. Toxicol. Program Tech. Rep. Ser.* **243**, 1–174.

Penaloza, C. G., Estevez, B., Han, D. M., Norouzi, M., Lockshin, R. A., and Zakeri, Z. (2014). Sex-dependent regulation of cytochrome P450 family members Cyp1a1, Cyp2e1, and Cyp7b1 by methylation of DNA. *Faseb J.* **28**, 966–977.

Philip, B. K., Mumtaz, M. M., Latendresse, J. R., and Mehendale, H. M. (2007). Impact of repeated exposure on toxicity of perchloroethylene in Swiss Webster mice. *Toxicology* **232**, 1–14.

Rakhshandehroo, M., Knoch, B., Muller, M., and Kersten, S. (2010). Peroxisome proliferator-activated receptor alpha target genes. *PPAR Res.* **2010**, 1. pii: 612089.

Ramdhan, D. H., Kamijima, M., Yamada, N., Ito, Y., Yanagiba, Y., Nakamura, D., Okamura, A., Ichihara, G., Aoyama, T., and Gonzalez, F. J. (2008). Molecular mechanism of trichloroethylene-induced hepatotoxicity mediated by CYP2E1. *Toxicol. Appl. Pharmacol.* **231**, 300–307.

Ramdhan, D. H., Kamijima, M., Wang, D., Ito, Y., Naito, H., Yanagiba, Y., Hayashi, Y., Tanaka, N., Aoyama, T., Gonzalez, F. J., *et al.* (2010). Differential response to trichloroethylene-induced hepatosteatosis in wild-type and PPARa-humanized Mice. *Environ. Health Perspect.* **118**, 1557–1563.

Ripp, S. L., Overby, L. H., Philpot, R. M., and Elfarra, A. A. (1997). Oxidation of cysteine S-conjugates by rabbit liver microsomes and cDNA-expressed flavin-containing monooxygenases: Studies with S-(1, 2-dichlorovinyl)-L-cysteine, S-(1, 2, 2-trichlorovinyl)-L-cysteine, S-allyl-L-cysteine, and S-benzyl-L-cysteine. *Mol. Pharmacol.* **51**, 507–515.

Song, J. Z., and Ho, J. W. (2003). Simultaneous detection of trichloroethylene alcohol and acetate in rat urine by gas chromatography-mass spectrometry. *J. Chromatogr. B Analyt Technol. Biomed. Life Sci.* **789**, 303–309.

U.S. EPA. (2011a). Toxicological review of tetrachloroethylene (CAS No. 127-18-4). In *Support of Summary Information on the Integrated Risk Information System (IRIS)*. U.S. Environmental Protection Agency, Washington, DC.

U.S. EPA. (2011b). Toxicological review of trichloroethylene (CAS No. 79-01-6). In *Support of Summary Information on the Integrated Risk Information System (IRIS)*. U.S. Environmental Protection Agency, Washington, DC.

U.S. EPA. (2017). *EPA Names First Chemicals for Review under New TSCA Legislation*. Available at: https://www.epa.gov/newsreleases/epa-names-first-chemicals-review-under-new-tsca-legislation. Accessed May 19, 2017.

Venkatratnam, A., Furuya, S., Kosyk, O., Gold, A., Bodnar, W., Konganti, K., Threadgill, D. W., Gillespie, K. M., Aylor, D. L., Wright, F. A., *et al.* (2017). Collaborative cross mouse population enables refinements to characterization of the variability in toxicokinetics of trichloroethylene and provides genetic evidence for the role of ppar pathway in its oxidative metabolism. *Toxicol. Sci.* **158**, 48–62.

Volkel, W., and Dekant, W. (1998). Chlorothioketene, the ultimate reactive intermediate formed by cysteine conjugate beta-lyase-mediated cleavage of the trichloroethene metabolite S-(1, 2-Dichlorovinyl)-L-cysteine, forms cytosine adducts in organic solvents, but not in aqueous solution. *Chem. Res. Toxicol.* **11**, 1082–1088.

Werner, M., Birner, G., and Dekant, W. (1996). Sulfoxidation of mercapturic acids derived from tri- and tetrachloroethene by cytochromes P450 3A: A bioactivation reaction in addition to deacetylation and cysteine conjugate beta-lyase mediated cleavage. *Chem. Res. Toxicol.* **9**, 41–49.

White, I. N., and De Matteis, F. (2001). The role of CYP forms in the metabolism and metabolic activation of HCFCs and other halocarbons. *Toxicol. Lett.* **124**, 121–128.

Yoo, H. S., Bradford, B. U., Kosyk, O., Shymonyak, S., Uehara, T., Collins, L. B., Bodnar, W. M., Ball, L. M., Gold, A., and Rusyn, I. (2015). Comparative analysis of the relationship between trichloroethylene metabolism and tissue-specific toxicity among inbred mouse strains: Liver effects. *J. Toxicol. Environ. Health A* **78**, 15–31.

Yoo, H. S., Bradford, B. U., Kosyk, O., Uehara, T., Shymonyak, S., Collins, L. B., Bodnar, W. M., Ball, L. M., Gold, A., and Rusyn, I. (2015). Comparative analysis of the relationship between trichloroethylene metabolism and tissue-specific toxicity among inbred mouse strains: Kidney effects. *J. Toxicol. Environ. Health A* **78**, 32–49.

Yoo, H. S., Cichocki, J. A., Kim, S., Venkatratnam, A., Iwata, Y., Kosyk, O., Bodnar, W., Sweet, S., Knap, A., Wade, T., *et al.* (2015). The contribution of peroxisome proliferator-activated receptor alpha to the relationship between toxicokinetics and toxicodynamics of trichloroethylene. *Toxicol. Sci.* **147**, 339–349.

Yue, F., Cheng, Y., Breschi, A., Vierstra, J., Wu, W., Ryba, T., Sandstrom, R., Ma, Z., Davis, C., Pope, B. D., *et al.* (2014). A comparative encyclopedia of DNA elements in the mouse genome. *Nature* **515**, 355–364.

Zhou, Y. C., and Waxman, D. J. (1998). Activation of peroxisome proliferator-activated receptors by chlorinated hydrocarbons and endogenous steroids. *Environ. Health Perspect.* **106**, 983–988.

Zhou, Y. H., Cichocki, J. A., Soldatow, V. Y., Scholl, E. H., Gallins, P. J., Jima, D., Yoo, H. S., Chiu, W. A., Wright, F. A., and Rusyn, I. (2017). Comparative dose-response analysis of liver and kidney transcriptomic effects of trichloroethylene and tetrachloroethylene in B6C3F1 mouse. *Toxicol. Sci.* **160**, 95–110.